PROCEEDINGS OF THE EUROPEAN CONFERENCE ON ENERGY DISPERSIVE X-RAY SPECTROMETRY 1998
Ed. J.E. Fernández and A. Tartari

DIFFUSION OF PHOTONS IN THE FRAME OF THE INTEGRAL FORM OF THE TRANSPORT EQUATION*

J.E. FERNANDEZ*, V.G. MOLINARI AND F. TEODORI
Laboratory of Montecuccolino, DIENCA, University of Bologna and Istituto Nazionale per la Fisica della Materia (INFM), via dei Colli 16, 40136 Bologna

In this paper the 3D photon transport equation is considered to give a detailed description of the fluorescence photon emission from a homogeneous slab. As an example we study, with a complete 3D spatial description in plane geometry, the distribution both in physical and momentum space of the primary photons, induced by a radiation beam crossing the slab. Then we will see how the 3D geometry influences the shape of the continuous spectra due to a second Compton collision which modifies the distribution of the primaries due to photoelectric effect. The possibility of isolating the effect of a particular interaction is one of the strength points of the multiple-scattering scheme in the framework of transport techniques, which allows a better understanding of the photon diffusion. In order to evaluate the effects of the boundary conditions, we will use the integral transport equation instead of the integro-differential one, which has the advantage of treating the flow of the photons from the outer space as an external source. The results will be compared with those obtained in the case of a half-infinite medium uniformly irradiated with a plane infinite slant source of monochromatic photons previously solved in 1D.

INTRODUCTION

It is well known that in many practical situations, the radiation field can be considered a dynamic system composed of mass-less, classical, point particles, which interact individually with the matter and, between an interaction and another, move in straight line with the speed of light. In this situation all the radiation properties of main interest can be calculated, when the angular flux is known, by expressing the rate of photon flow per unit solid angle, unit wavelength and unit time, through a unit surface normal to the travelling direction. It is also known that the angular flux can be calculated by solving the stationary equation of transfer[1,2]

$$-\dot{\omega}\cdot\vec{\nabla}f(\vec{r},\dot{\omega},\lambda)-\mu(\vec{r},\lambda)\,f(\vec{r},\dot{\omega},\lambda)+\int_0^{\infty}d\lambda'\int_{4\pi}d\dot{\omega}'K(\vec{r},\dot{\omega}\cdot\dot{\omega}',\lambda'\rightarrow\lambda)f(\vec{r},\dot{\omega}',\lambda')+q(\vec{r},\dot{\omega},\lambda)=0 \quad [1]$$

which is a generalisation of the Boltzmann equation, widely used in particle transport theory. Into it, $\mu(\vec{r},\lambda)$ is the linear attenuation coefficient, $K(\vec{r},\dot{\omega}\cdot\dot{\omega}',\lambda'\rightarrow\lambda)$ is the interaction kernel and $q(\vec{r},\dot{\omega},\lambda)$ is the external source.

In general, to find the exact solution is out of question. A very useful approach consists in building up a Neuman type series solution with the powers of the equation kernel. From a physical point of view, it is a matter of calculating the angular flux of the unscattered photons, of the once-scattered photons and so on. Due to the notable physical meaning of the terms, even if the complete solution can not be found, the equation constitutes a very good instrument of analysis to study the effects on the radiation of the interactions with the matter.

In some previous works[3,4] the multiple-scattering scheme technique was successfully applied to investigate the properties of the radiation reflected by a half-infinite medium uniformly irradiated by a plane, slant, monochromatic and unidirectional source. The results shown with great extent of detail the influence of the photoelectric effect, and of the Compton and Rayleigh scattering (the most important interaction processes in the X-ray regime) to build up the fluorescence spectrum.
In this work, we want to analyse the radiation field produced by a narrow monochromatic photon beam, which crosses through a homogeneous and isotropic slab. It is easy to understand that, in such a situation, not only the interactions, but also the peculiarity of the geometry and the boundary conditions play a major role, reason why the use of the equation of transfer in integral form is preferable:

$$f(\vec{r}, \hat{\omega}, \lambda) = \Gamma(\vec{r}_e, \hat{\omega}, \lambda) \cdot \exp\left[-\int_0^{|\vec{r}_e - \vec{r}|} ds\mu\ (\vec{r} - \hat{\omega}s, \lambda)\right] + \int_0^{|\vec{r}_e - \vec{r}|} ds' q\ (\vec{r} - \hat{\omega}s', \hat{\omega}, \lambda) \exp\left[-\int_0^{s'} ds''\mu\ (\vec{r} - \hat{\omega}s'', \lambda)\right] +$$

$$+ \int_0^{|\vec{r}_e - \vec{r}|} ds' \int_0^{\infty} d\lambda' \int_{4\pi} d\hat{\omega}' K(\vec{r} - \hat{\omega}s', \hat{\omega} \cdot \hat{\omega}', \lambda' \rightarrow \lambda) f(\vec{r} - \hat{\omega}s', \hat{\omega}, \lambda') \exp\left[-\int_0^{s'} ds''\mu\ (\vec{r} - \hat{\omega}s'', \lambda)\right] \quad [2]$$

In (2), $\Gamma(\vec{r}_e, \hat{\omega}, \lambda)$ is the angular flux evaluated at the intersection point $\vec{r}_e$ of the external surface with the straight line $\vec{r}_e - s\hat{\omega}$.

RESULTS AND DISCUSSION

The interactions, that we want to consider for the example, are the Compton scattering and the photoelectric effect; thus the kernel of the equation is composed of two terms. The first one is the differential Compton cross section, given by

$$\sigma(\hat{\omega} \cdot \hat{\omega}', \lambda' \rightarrow \lambda) = S(\lambda', \hat{\omega} \cdot \hat{\omega}', Z)\ K(\lambda, \lambda')\ \delta(1 + \lambda' - \lambda - \hat{\omega} \cdot \hat{\omega}') \quad [3]$$

where[5,6]

$$K(\lambda, \lambda') = \frac{r_0^2}{2} \left(\frac{\lambda'}{\lambda}\right) \left(\frac{\lambda}{\lambda'} + \frac{\lambda'}{\lambda} + (\lambda - \lambda')(\lambda - \lambda' - 2)\right) \quad [4]$$

and $S(\lambda', \hat{\omega} \cdot \hat{\omega}', Z)$ is the atomic form factor,[7] which takes into account the effects of the electron binding. The electron motion before the scattering is neglected, so the Compton peak is limited to a monochromatic line. The second term is the photoelectric differential cross section[8-10]

$$\sigma(\omega \cdot \omega', \lambda' \rightarrow \lambda) = \sum_i \frac{1}{4\pi} Q_{\lambda_i}(\lambda')\ \delta(\lambda - \lambda_i)\ U(\lambda_{e_i} - \lambda') \quad [5]$$

where Q_{λ_i} denotes the emission probability for the i-th line. Due to the geometry of the problem we choose a cylindrical coordinates system with Z-axis along the beam and origin at the hitting point on the bounding surface (Figure 1). By denoting

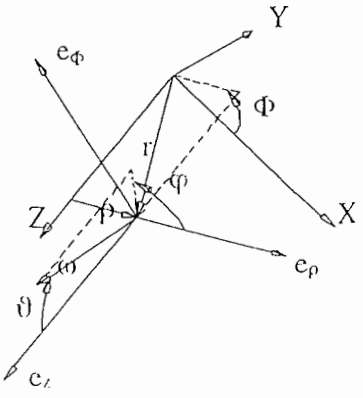

Fig. 1. Cylindrical coordinates system.

$$\vec{n} = \text{sen}\,\theta_0 \cos\varphi_0 \vec{e}_x + \text{sen}\,\theta_0\,\text{sen}\,\varphi_0 \vec{e}_y + \cos\theta_0 \vec{e}_z \qquad [6]$$

the unit vector normal to the external surface, such that $\vec{n} \cdot \vec{\omega} \geq 0$, and a the slab thickness, the following transport equation results:

$f(\rho, z, \Phi, \lambda) =$

$$= \left\{ U(\text{sen}\,\vartheta\,\text{sen}\,\vartheta_0 \cos(\Phi+\varphi-\varphi_0) + \cos\vartheta\cos\vartheta_0) \int_0^{\frac{\rho\,\text{sen}\,\vartheta_0\cos(\Phi-\varphi_0)+z\cos\vartheta_0}{\text{sen}\,\vartheta\,\text{sen}\,\vartheta_0\cos(\Phi+\varphi-\varphi_0)+\cos\vartheta\cos\vartheta_0}} ds + \right.$$

$$\left. + U(-\text{sen}\,\vartheta\,\text{sen}\,\vartheta_0 \cos(\Phi+\varphi-\varphi_0) - \cos\vartheta\cos\vartheta_0) \int_0^{\frac{\rho\,\text{sen}\,\vartheta_0\cos(\Phi-\varphi_0)+z\cos\vartheta_0-a}{\text{sen}\,\vartheta\,\text{sen}\,\vartheta_0\cos(\Phi+\varphi-\varphi_0)+\cos\vartheta\cos\vartheta_0}} ds \right\} \cdot$$

$$\int_{4\pi} d\bar{\omega}' \int_0^{\infty} d\lambda' N \left[S(\lambda', 1+\lambda'-\lambda, Z) K(\lambda, \lambda') \delta\left(1+\lambda'-\lambda - \frac{\rho\cos(\varphi-\varphi') - s\,\text{sen}\,\vartheta\cos\varphi'}{\sqrt{\rho^2+s\,\text{sen}^2\,\vartheta - 2\rho s\,\text{sen}\,\vartheta\cos\varphi}} \text{sen}\,\vartheta\,\text{sen}\,\vartheta' - \cos\vartheta\cos\vartheta' \right) + \right.$$

$$\left. + \sum_i U(\lambda_{ei} - \lambda') Q_{\lambda_i}(\lambda') \delta(\lambda - \lambda_i) \frac{1}{4\pi} \right] \cdot$$

$$\cdot f\left(\sqrt{\rho^2 + s^2\,\text{sen}^2\,\vartheta - 2\rho s\,\text{sen}\,\vartheta\cos\varphi}, z - s\cos\vartheta, a\tan\frac{\rho\,\text{sen}\,\Phi - s\,\text{sen}\,\vartheta\,\text{sen}(\Phi+\varphi)}{\rho\cos\Phi - s\,\text{sen}\,\vartheta\cos(\Phi+\varphi)}, \cos\vartheta', \varphi', \lambda' \right) \exp[-\mu(\lambda)s] +$$

$$+ \left\{ U(\text{sen}\,\vartheta\,\text{sen}\,\vartheta_0 \cos(\Phi+\varphi-\varphi_0) + \cos\vartheta\cos\vartheta_0) \int_0^{\frac{\rho\,\text{sen}\,\vartheta_0\cos(\Phi-\varphi_0)+z\cos\vartheta_0}{\text{sen}\,\vartheta\,\text{sen}\,\vartheta_0\cos(\Phi+\varphi-\varphi_0)+\cos\vartheta\cos\vartheta_0}} ds \right.$$

$$\left. + U(-\text{sen}\,\vartheta\,\text{sen}\,\vartheta_0 \cos(\Phi+\varphi-\varphi_0) - \cos\vartheta\cos\vartheta_0) \int_0^{\frac{\rho\,\text{sen}\,\vartheta_0\cos(\Phi-\varphi_0)+z\cos\vartheta_0-a}{\text{sen}\,\vartheta\,\text{sen}\,\vartheta_0\cos(\Phi+\varphi-\varphi_0)+\cos\vartheta\cos\vartheta_0}} ds \right\} \cdot$$

$$\cdot I_0 \frac{\delta\left(\sqrt{\rho^2+s^2\,\text{sen}^2\,\vartheta - 2\rho s\,\text{sen}\,\vartheta\cos\varphi}\right)}{r} \delta(z - s\cos\vartheta)\delta(\cos\vartheta - 1)\delta(\lambda - \lambda_0)\exp[-\mu(\lambda_0)s] \qquad [7]$$

In spite of the adoption of a cylindrical coordinates system, it keeps the same standard form. The only problem has been to express the term $r - s\vec{\omega}$ and to evaluate the effects of the angular redistribution on the term $\vec{\omega} \cdot \vec{\omega}'$.

To simplify, we supposed the medium to be composed of only one specimen, whose density is N atoms per unit volume. Due to its linearity, the equation can be easily generalised to treat composite materials.

Using this equation, we have determined the distribution, both in physical and momentum space, of the Compton and photoelectric primary photons; then we have studied the changes that a further Compton interaction produces on the profile of the primary photons generated by photoelectric effect. We obtained an analytical solution, which is at all general and able to give a great amount of information on the radiation field. By it, we derived the angular distribution of the photoelectric-Compton photons that come out from a generic point on the surface of the slab with any energy. Some of the results are illustrated in the polar diagrams reported below. To interpret them one must refer to figure 2 which shows the geometry of the problem.

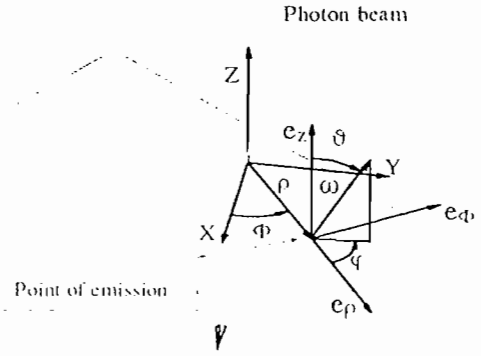

Fig. 2. Laboratory Coordinates System.

In the calculation, we supposed a beam of 10 keV with an inclination angle of 1 radian with respect to the normal to the slab surface. The material is supposed to be aluminium, which has an emission line of 1.487 keV in the range, we are interested to. The radiation, we have chosen to observe, has an energy of 1.485 keV, that is to say, we want to study those photons, that after a Compton interaction have undergone a deflection of $\pi/3$ radians.

In the diagrams we have reported the quantity $\int_{\Delta\theta\Delta\varphi\omega} d\dot{\omega} f(\vec{r}, \dot{\omega}, \lambda)/(\Delta\theta\Delta\varphi)$, where $\Delta\dot{\omega}(\dot{\omega})$ is the elementary solid angle around $\dot{\omega}$. In particular we chose $\Delta\varphi = 2\pi/100$ and $\Delta\theta = \pi/100$.

The first two representations (Figs. 3 and 4) are referred to an emission point positioned on the z-beam plane, by using other words, a point whose azimuth is $\Phi = 0$. The shape of the 3D surfaces shows that the prevalent contribution is due to the fluorescence radiation produced near the beginning of the beam path through the slab. This is easily understandable because both the photoelectric productions and the escape probability decrease with the depth. The spread of the radiation around the z-beam plane puts in evidence the effect of the Compton interaction (undergone before leaving the slab) on the angular distribution.

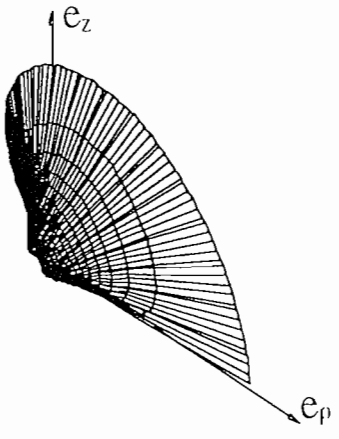

Fig. 3. Emission point $\Phi = 0$. 3D view.

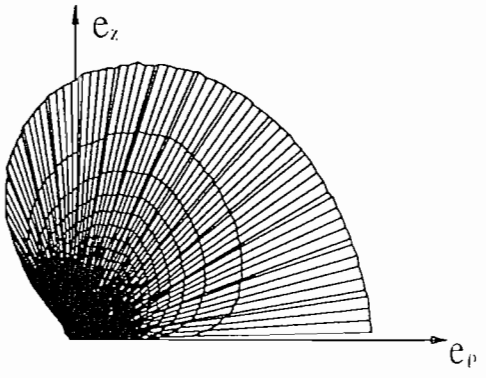

Fig. 4. Emission point $\Phi = 0$. Left view.

The next two graphical representations (Figs. 5 and 6) are referred to an emission point on the plane, whose equation is $\Phi = 3\pi/2$. The first thing that we can note is the obvious absence of a symmetry plane. By examining the two of series of graphics, we see that Compton scattering determines a full 3D angular dispersion of the photons, which, without having interacted, should move on the beam plane by the emission point. In spite of this, only one Compton deflection is not enough to get the photons to completely forget the source geometrical dislocation. This is the reason why the graphical representations show a maximum of emission when the travelling direction lays on the beam plane. In other words, in spite of the spread due to the Compton deflections, the distribution of the secondary photons still reflects the geometry of the source.

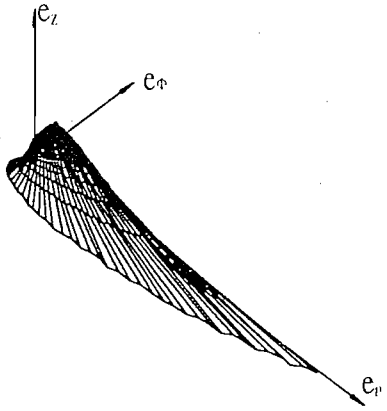

Fig. 5. Emission point $\Phi = 3\pi/2$. 3D view.

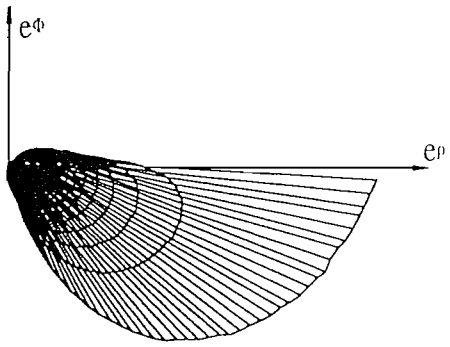

Fig. 6. Emission point $\Phi = 3\pi/2$. Top view.

So far we studied the angular distribution of photons which had a well defined energy. Now we reverse the problem and analyse the energetic spectra of the photoelectric-Compton photons emitted with a given travelling direction. It is worth to remember that the (P,C) continuous distribution is responsible for the asymmetry of the characteristic lines,[11] and therefore, has important consequences on the modelling and measurement of these lines.[12] Our 3D solution predicts the results reported in the figures 7, 8 and 9. Obviously these cases cannot exhaust all the possible situations.

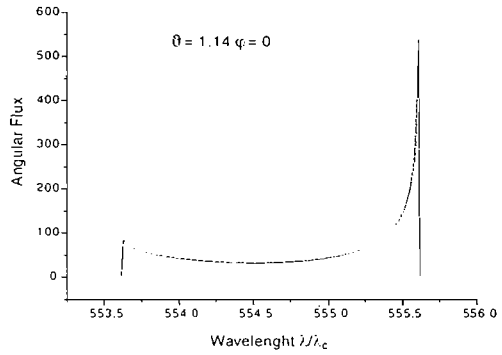

Fig. 7. Energy distribution of the photons from a point at azimuth $\Phi = 0$.

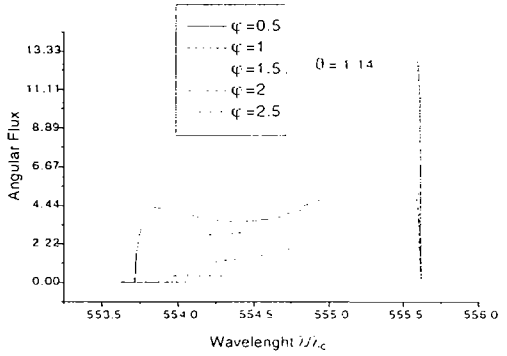

Fig. 8. Energy distributions of photons from a point at azimuth Φ=0. A sampling has been made of the possible travelling directions of the photons.

However they illustrate the relation which links among them, the emission point, the observation angle, and the properties of the radiation detected, when the geometry of the system is not simple. All the curves, with the exception of figure 7, show a high energy cut. This is a peculiar geometrical effect, due to the fact that the primary source is well localised along the beam trajectory and that the slab thickness is finite. Thus, the contributions to the Compton collision in all the positions outside the beam trajectory, cannot receive anymore photoelectric emissions from the whole 4π directions, and the spectrum width becomes lower than $2\lambda_c$. In contrast, the spectrum reported in figure 7 –maximum width– corresponds to detection (observation) with a direction which intersects the trajectory of the source beam (and therefore, the distribution of photoelectric centres).

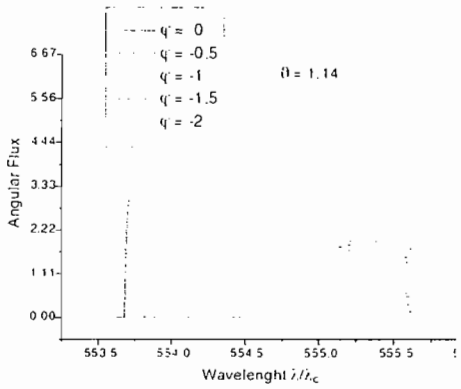

Fig. 9. Energy of photons from a point at azimuth $\Phi=3\pi/2$. Again a sampling has been made of the possible travelling directions of the photons.

CONCLUSIONS

In this paper, we tested with success the possibility of attacking with analytical techniques the Boltzmann equation for systems with more complex source distributions than the plane one. The reported test case illustrate and underline the great descriptive power of the solution we found, and what a valid analysis tool the transport equation is to reach a profound understanding of the fundamental aspects of the photon diffusion phenomena and to better interpret the experimental results. The results stress the importance of 3D modelling to describe appropriately the effect of a realistic geometry like a narrow beam on the X-ray fluorescence spectrum.

Thus far our results have been obtained within the framework of the Boltzmann transport theory, neglecting polarisation. That is to say, we evaluated the angular flux using interaction kernels averaged over the polarisation states. It is known that the scattering of the unpolarised photons produces a partially polarised radiation with a fraction of linearly polarised photons.[13,14] It is also known that polarised radiation can be treated with the transport theory, by replacing the scalar Boltzmann equation with a set of four equations of transfer coupled by the in-scattering term.[2,13] In the future we intend to remove this approximation to investigate the role of the geometrical set-up in combination with the effects of the polarisation on the diffusion of photons, using multiple scattering techniques.

REFERENCES

1. Fano U., Spencer L.V. and Berger M.J., Penetration and diffusion of X-rays, in: *Handbuch der Physik*, S. Flugge (Ed.) vol. XXXVIII/2, pp. 660-817, Springer (Berlin, 1960).
2. Pomraming G. C., *The equations of radiation hydrodynamics*, Pergamon Press (Oxford, 1973).
3. Fernández J.E. and Molinari V.G., X-ray photon spectroscopy calculations, in *Advances in Nuclear Science and technology*, J. Lewins (Ed.) vol. 22, Plenum Press (New York, 1991)
4. Fernández J.E., Molinari V.G. and Sumini M., Effect of the X-ray scattering anisotropy on the diffusion of photons in the frame of transport theory, *Nucl. Instrum. Methods* **A280** 212-221 (1989).
5. Klein O. and Nishina Y., Uber die streuung von strahlung durch freie elektronen nach der neuen relativistischen quantendynamik von Dirac, *Z. Phys.* **52**, 853 (1929)
6. Evans R.D., Compton effect, in: *Handbuch der Physik*, S. Flugge (Ed.) vol XXXIV, p. 218, Springer (Berlin, 1958).
7. Hubbell J.H., Veigele W.J., Briggs E.A., Brown R.T., Cromer D.T. and Howerton R.J., Atomic form factors, incoherent scattering functions and photon scattering cross- sections, *J. Phys. Chem. Ref. Data* **4**, 471 (1975).
8. Fernández J.E., XRF intensity in the frame of the transport theory, *X-Ray Spectrom.* **18**, 271 (1989).
9. McMaster W.H., Kerr del Grande N., Mallet J.H. and Hubbell J.H., *Compilation of X-ray cross-sections*, Lawrence Livermore National Laboratory Report UCRL-50174, Section 2, Rev. I (1969).
10. Scofield J.H., *Theoretical photo-ionization cross-sections from 1 to 1500 keV*, Lawrence Livermore National Laboratory Report UCRL-51326 (1973).
11. Fernández J.E., Rayleigh and Compton scattering contributions to X-ray fluorescence intensity, *X-Ray Spectrom.* **21**, 57-68 (1992).
12. Kis-Varga M. and Végh J., Influence of in-sample scattering of fluorescent radiation on line shapes of Si(Li) detectors in XRF studies, *X-Ray Spectrom.* **22**, 166-171 (1993).
13. Fernández J.E. and Molinari V.G., Diffusion of polarized photons in the frame of transport Theory, *Nucl. Instrum. Methods* **B73**, 341-351 (1993).
14. Fernández J.E., Hubbell J.H., Hanson A.L. and Spencer L.V., Polarization effects on multiple scattering gamma transport, *Rad. Phys. Chem.* **41**, 579-630 (1993).

* Corresponding author. E-mail: jorge.fernandez@mail.ing.unibo.it

* A more detailed version of this article is being considered for publication in the journal *X-Ray Spectrometry*, the copyright of this article is owned by John Wiley & Sons.